RUSSIAN JOURNAL OF EARTH SCIENCES, VOL. 10, ES5002, doi:10.2205/2008ES000303, 2008

Analysis of seismicity in North India

V. Gitis,[1] E. Yurkov,[1] B. Arora,[2] S. Chabak,[2] N. Kumar,[2] and P. Baidya[3]

Received 4 June 2008; accepted 10 June 2008; published 18 June 2008.

[1] The geotectonic information on North India region has been processed using GIS (Geographic Information Systems), GeoProcessor for extracting the spatial seismotectonic properties. According to spatial modeling of the principle seismotectonic parameters the region under study can be divided into four zones as Kangra-Chamba, Garhwal-Kumaon, Punjab reentrant and Delhi-Haridwar. The *b*-value is low (0.5) for the Kangra-Chamba and Garhwal-Kumaon region, which shows that the regions have less capacity to withstand the developing stress. The elliptical region between Main Central thrust (MCT) and Main Boundary Thrust (MBT) are sensitive to the tidal force. *INDEX TERMS:* 0500 Computational Geophysics; 0530 Computational Geophysics: Data presentation and visualization; 7230 Seismology: Seismicity and tectonics; 8010 Structural Geology: Fractures and faults; *KEYWORDS:* seismicity, tectonics, geographic information systems, Himalaya.

Citation: Gitis, V., E. Yurkov, B. Arora, S. Chabak, N. Kumar, and P. Baidya (2008), Analysis of seismicity in North India, *Russ. J. Earth. Sci., 10,* ES5002, doi:10.2205/2008ES000303.

1. Introduction

[2] Since last 20 years, the Wadia Institute of Himalayan Geology (WIHG), Dehradun, India has been supporting the multidisciplinary research in exploring the structure and history of the Himalaya based on seismotectonic investigations. The institute has collected a complementary dataset of geophysical time series at different locations in Northern India (26°–34°N and 74°–82°E) containing the information of seismology, tectonics deformation. The Himalaya region has many thrust faults capable of producing the earthquakes of magnitude 8.0 or greater. Some of these faults are very prominent and visible at the surface but some faults are hidden. These faults are mostly concentrated in the mountain region producing hundreds of earthquakes every year though most are too small to detect. Recently an earthquake of $M = 7.6$ occurred at Muzzfrabad on 8 October 2005 at northwest boundary of present study region [*Rao et al.,* 2006].

[3] Himalaya, the arcuate mountain belt of complex geotectonic setup stretching about 2400 km long in east-west direction with variable width of 230 to 320 km is formed due to the convergent movement of two plates of the earth's lithosphere. The Indian and Asian continental plates collided some 50 m.y. ago [*Le Fort,* 1975] resulting lithosphere deformation and modification of the seismotectonic model of the region with the span of time. The seismotectonic investigations have been done by many authors [*Seeber and Armbruster,* 1981; *Ni and Barazangi,* 1984; *Thakur and Kumar,* 2002; *Kayal,* 2007; *Bollinger et al.,* 2007; *Kumar et al.,* 2008, (in press)] and for the region of NW Himalaya; we have well documented information of great ($M \geq 8.0$) seismic events since 1551 and geotectonic information of last two centuries. To understand the ongoing deformation pattern of Himalaya, *Seeber and Arnbruster* [1981] proposed a steady state tectonic model while *Ni and Barazangi* [1984] formulated an evolutionary model. These models have highlighted the seismogenic discontinuities as MBT, MCT, a plane of detachment (MBT and MCT coincide with this plane at depth) and the Basement thrust. Most of the seismicity lies between MBT and MCT and steady state model states that both these thrusts are active but MCT is evaluated as inactive in the evolutionary model.

[4] This work addresses the results on development of geoinformation technology oriented to seismotectonic problem domain [*Gitis and Ermakov,* 2004] and application of the technology to spatial analysis of seismicity in North India region.

[5] Web-GIS GeoProcessor 1.5 [*Gitis et al.,* 1998; *Gitis,* 2004] and GIS SeismoTide [*Yurkov and Gitis,* 2005] were used. Further we will consider the initial data and geoinformation tools, after then we present three main results of data exploration: spatial patterns of main seismic parameters, some relationships between seismicity and components of tidal force, and spatial analysis of relationship between strong earthquakes with $M \geq 6.0$ and digital elevation model.

[1]Institute for Information Transmission Problems, RAS, Moscow, Russia
[2]Wadia Institute of Himalayan Geology, Dehradun, India
[3]India Meteorological Department, New Delhi, India

Copyright 2008 by the Russian Journal of Earth Sciences.
ISSN: 1681–1208 (online)

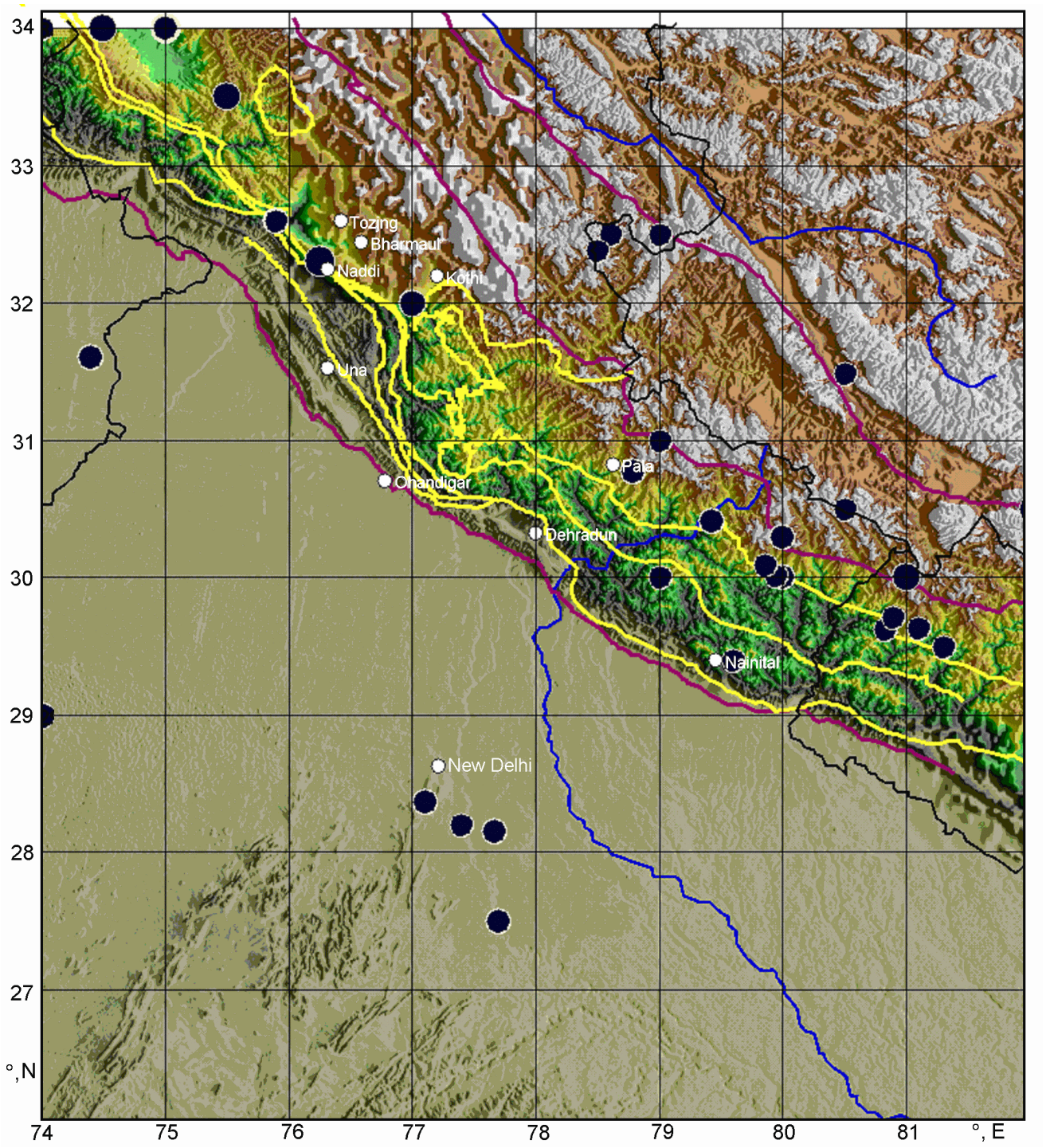

Figure 1. Seismotectonic model of North India region. Circles are earthquakes $M \geq 6.0$ from 1552 till 30.01.2005, yellow lines are active thrusts, red lines are tectonic faults, lilac lines are non active thrusts, black lines are National boundaries.

2. Geotectonic Model of North India Region

[6] Himalaya is the result of convergent movement of Indian plate moving to the northward and under thrusting to the south moving Eurasian plate (Figure 1). The result of this convergence has formed the arcuate mountain belt, stretching from Nanga Parbat in the west to the Namche Barwa in the east. The collision of these two plates has formed the widespread Tertiary transgressions and development of major thrusts and nappes, directed towards

the converging plate (Indian subcontinent). It is the earth's largest and youngest mountain range comprising the rock types from the Palaeoproterozoic to the Quaternary age. Its northern margin is demarcated by the Indus-Tsangpo Suture zone (ITSZ) and the southern margin by the Indo-Gangetic plains. In north-south direction, the Himalaya can be divided geotectonically into four parallel zones by the four principal intracrustal thrust. The Himalayan Frontal thrust (HFT), the Main Boundary Thrust (MBT), the Main Central Thrust (MCT) and the ITSZ are the major tectonic discontinuities, which separate these zones from each other.

[7] The HFT or MFT (Main Frontal Thrust) is the southern most, younger and neotectonically active thrust of the Himalayan region giving a topographical break of the Himalaya (the Outer Himalaya), against the alluvial Indo-Gangetic Plains. The Outer Himalaya comprises the low altitude Siwalik Hills with flat-floored structural valleys consisting of about 9500 m thick Cenozoic sedimentary pile characterized by folds and faults [*Thakur,* 1992]. The Indo-Gangetic plains of thick alluvial lie to the south of this discontinuity that is formed due to thick deposited sediments by the Indus, the Ganga and other Rivers. The Delhi-Hardwar ridge is the important structural feature in the Ganga basin which is tectonically and seismically active as compared to the rest of the basin.

[8] The evolutionary model of Himalaya [*Le Fort,* 1975] states that MBT is the younger tectonic discontinuity as compare to MCT, which is more active currently. However, both the MCT and MBT has been treated as the contemporaneous features in the steady-state model of *Seeber and Armbruster* [1981] and these merge with each other at depth with a common detachment surface. The MBT is the tectonic boundary between the Lesser Himalaya nappes lying to its north and the Tertiaries of the Outer Himalaya foreland basin to the south. The majority of the earthquakes in the NW Himalaya are concentrated in the zone between MBT and MCT of shallow focal depth and great Himalayan earthquakes are originated at the surface of the detachment, which represents the upper surface of the underthrusting Indian plate with apparent northward dip of about 15°[*Ni and Barazangi,* 1984].

[9] The MCT is the major tectonic discontinuity, which divide the two contrasting structures as Lesser and Higher Himalaya having contrasting stratigraphic and tectonic features. The relative movement of the blocks across this tectonic discontinuity has caused the development of crustal buckles in which the Palaeogene and Neogene sediments have deposited. At depth the MCT represents a ductile shear zone and tectonically it is a duplex shear zone having three distinct thrust planes as MCT I, MCT II and MCT III. According to the degree of metamorphism, lithostratigraphy and tectonic setting, Valdiya (1980) has named these thrusts as Chail (MCT I, lower thrust), Jutogh (MCT II, middle thrust) and Vaikrita (MCT III, upper thrust).

[10] The ITSZ is the discontinuity along which the initial contact between the two plates occurred in the Early Eocene (60-70 my ago). The Tethys Sea, which was existed between two continents, vanished to the end of Eocene and after that the ITSZ converted to active plate boundary. The region between ITSZ and the MCT is composed of the Tethyan sedimentary zone in the north and the central crystalline zone in the south. The suture is made up of imbricated mélanges of flysch sediments, pillow lavas, volcanics and the basic and ultrabasic rocks, which are cut by steep faults [*Allegre et al.,* 1984]. According to *Burg et al.,* [1984], the Tethyan slab consists of several thrust sheets with distinct ages and deformations. Mainly normal faulting is existed in the high Himalaya and the normal fault zone separates the highly metamorphosed crystalline rock and a transitional zone from the overlying sedimentary sequence.

3. Initial Data Set and Geoinformation Modelling Tools

[11] The following initial data were used for geoinformation analysis: historical and instrumental earthquake catalogue of Wadia Institute of Himalayan Geology from 1552 till 30.01.2005, digital elevation model in grid $30'' \times 30''$, linear tectonic structures (active thrusts, non-active thrusts and faults), and astronomical data (right ascension and declination of moon).

[12] Geoinformation modeling tools were presented by Web-GIS GeoProcessor 1.5 and GIS SeismoTide.

[13] Web-GIS GeoProcessor 1.5 (http://www.iitp.ru/projects/geo) is implemented as Java 1.5 applet. The applet can be used for decision support in environmental zonation, natural hazard and risk assessment, and exploration of natural resources. The system provides the following facilities of complex geodata analysis:

- *Data access:* Compiling the GIS-projects getting the relevant geographical layers distributed in different web-servers and user's computer.
- *Cartography exploration:* Interactive composition of a map consisted of several vector and grid-based layers, scaling and pan with or without interpolation of grid-based layers, changing the color bar, reading grid-based data in arbitrary points, calculation, visualization and reading the values from a set of grid-based layer cross-sections along the arbitrary profiles, illumination modeling, composition of sample sets in the form of points or/and polygons, creation of the maps of similarity with precedents according to user defined set of grid-based layers.
- *Data transformation:* Generation of a new grid-based layer applying a set of transformations to the linear and point layers, with the help of grid-based data filtering, and constructing the user defined functions of several grid-based layers with a set of elementary functions, algebraic and logical operations.
- *Spatial plausible reasoning:* Estimation of empirical distribution function, estimation of similarity function with a set of precedents, estimation of similarity function based on expert knowledge, estimation of membership function for two classes.

[14] GIS SeismoTide operates in the Matlab environment. It was designed specially for calculating tidal force characteristics, assessing the measure of correlation between seismicity and tidal force, and composing the maps of prevailing seismic activity. Each element of such a map shows phases (positive or negative) of tidal force components corresponding to higher recurrence rates of earthquakes. These maps facilitate the identification of seismically sensitive areas to the tidal force. Detection of the area is based both on visual analysis of the prevailing seismicity spatial pattern and on a statistical measure relationship between the seismic activity predominance and the different tidal force phases.

4. Spatial Modelling of Seismological Parameters

[15] Earthquake catalogue of Wadia Institute of Himalayan Geology includes 2628 seismic events occurred from 1552 till 30.01.2005. Seismological network was significantly improved in 1988. Therefore 1856 earthquakes from 01.01.1999 till 30.01.2005 were used for spatial modeling.

[16] These data were used for compiling the following three grid based models:

1. Spatial model of sensitivity of North India Seismic Network,
2. Spatial model of b-value,
3. Spatial model of seismic activity.

[17] To compile the models the seismic data are scanned with moving spatio-temporal window. Seismic parameters are estimated by the earthquakes with the epicenters inside the window. Evidently, the accuracy of the estimates depends on a number of the epicenters. It is supposed that a set of epicenters inside the window is statistically uniform. For that the window must cover homogeneous area in seismotectonic sense. Increasing the window size leads to doubtful estimates because of mixing evidences from different probabilistic distributions. Decreasing the window leads to uncertainties because of a small number of a sample set. A compromise consists in adaptive fitting of the window size: the more density of seismic events the less the window size.

[18] Moving window in our case is a cylinder with fixed height equal temporal interval from 01.01.1999 till 30.01.2005 and with radius which adaptively varies from R_1 to R_2. Minimal number of seismic events in window $N_{\min}$ and nominal number of events N are specified.

[19] The adaptive window algorithm is in following. Axis of the cylinder coincide with a grid point (λ, φ, t). If a number of events in cylinder of radius R_1 is $n \geq N$ then estimation is made. If number of events in cylinder of radius R_2 is $n \leq N_{\min}$, then estimation is rejected. If number of events in cylinder of radius R_2 is $N_{min} \leq n \leq N$, then estimation is made. If number of events in cylinder of radius R_2 is $n > N$, then the N nearest events to the grid point (λ, φ, t) is selected.

[20] Minimal representative magnitude of earthquakes m_0 is the left boundary of the interval, in which Gutenberg-Richter low is hold. Value m_0 depends on number of seismic stations, their spatial distribution, and sensitivity. The method of estimation of m_0 is based on testing of statistical hypothesis. The method was developed by *Pisarenko,* [1989], algorithm was developed by *Smirnov,* [1995], and together with Smirnov was modified for GIS GeoTime [*Gitis et al.,* 1994].

[21] Spatial model of m_0 in grid $4' \times 4'$ is calculated with the parameters: R_1=50 km, R_2=200 km, $N_{\min} = 25$, $N = 75$. Grid-based model of m_0 was smoothed with moving window R=20 km (Figure 2).

[22] Maximum likelihood estimate of b-value is following:

$$b(\lambda, \varphi, t) = \beta(\lambda, \varphi, t) \lg e \approx 0.43\beta(\lambda, \varphi, t),$$

where $\beta(\lambda, \varphi, t) = (\frac{1}{N_{m_0}} \sum m_i \geq m_0(m_i - m_0(\lambda, \varphi, t)))^{-1}$, $N_{m_0} = N_{m_0}(\lambda, \varphi, t)$ is a number of earthquakes with $m \in (m_0(\lambda, \varphi, t), M_{\max}(\lambda, \varphi, t))$.

[23] Spatial model of b-value in grid $4' \times 4'$ is calculated with the parameters: R_1=50 km, R_2=120 km, $N_{\min} = 20$, $N = 70$. Grid-based model of b-value smoothed with moving window R=20 km is represented at Figure 3.

[24] Seismic activity $A(\lambda, \varphi, t)$ is defined as normalized according to spatio-temporal window, the number of earthquakes adjusted to the magnitude $m \in (m_A - \frac{\delta m}{2} < m_A + \frac{\delta m}{2})$

$$A(\lambda, \varphi, t) =$$
$$kN_{m_0}(\lambda, \varphi, t)[\exp(-\beta(\lambda, \varphi, t)(m_A - \frac{\delta m}{2} - m_0(\lambda, \varphi, t)))$$
$$- \exp(-\beta(\lambda, \varphi, t)(m_A + \frac{\delta m}{2} - m_0(\lambda, \varphi, t))),$$

where $N_{m_0}(\lambda, \varphi, t)$ is a number of earthquakes with the magnitudes $m \in (m_0(\lambda, \varphi, t), M_{\max}(\lambda, \varphi, t))$, $k = 1/ST$, S is a spatial size of the window, T is the temporal interval of the window.

[25] Spatial model of seismic activity in grid $4' \times 4'$ is calculated with the parameters: R_1=50 km, R_2=120 km, $N_{\min}$=20, N=70. Grid-based model of seismic activity smoothed with moving window R=20 km is represented at Figure 4.

5. Relationship Between Seismicity and Components of Tidal Force

[26] Relationship between tidal force and frequency of earthquakes was investigated. Tidal force was calculated from a model of the gravitational interaction between the Earth and Moon. We neglect the solar component of the tidal force because, on average, it is more than two times less of the lunar component. The disregard of this component does not hinder the establishment of the fact of existence of statistical relations between seismicity and earth tides.

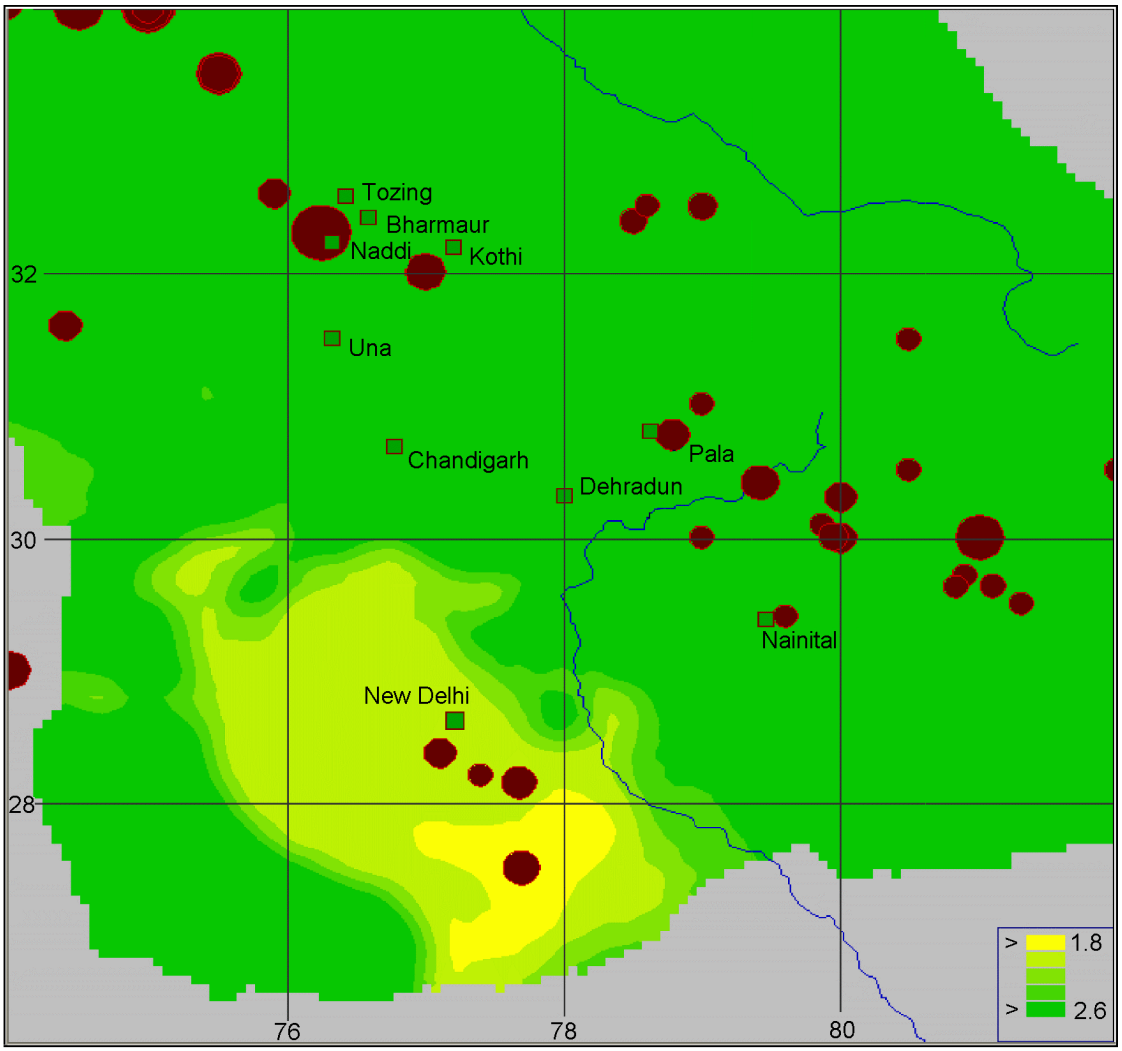

Figure 2. Spatial pattern of minimal representative magnitudes estimated by the WIHG earthquake catalogue from 01.01.1999 – 30.01.2005.

[27] Astrometry data were used for synchronization of tidal force with earthquakes. Characteristics of tidal force were examined: vertical (radial) component F_{r}, north-south F_{SN} and east-west F_{WE} horizontal components, the module of a vector of horizontal components F_{h} and the module of the full vector of tidal force $|F|$. Time diagrams of tidal vector components for latitude 320 are shown on Figure 5. In figure we see fast components with daily and semidiurnal the periods and slow a components with the fortnightly period. On the top of the diagram a dashed line shows envelope A_{r} for characteristic F_{r}. This characteristic we shall name a daily variation of tidal force.

[28] Two phases: positive ("+") and negative ("–") were considered for each characteristic of tidal force. The phase was considered positive if the characteristic exceeds its average value for the long-term period. Otherwise the phase was considered negative. The phase changes a sign one or two times per day for the first five characteristics and two times per month for the daily variation A_{r}. Duration of each phase depends on a sort of the characteristic and from latitude of a place of supervision and does not depends on a longitude.

[29] For revealing correlations between seismicity and tidal force the special statistical measure was used

$$s = \frac{f_+ - f_-}{\sqrt{\frac{f_+}{T_-} + \frac{f_-}{T_+}}},$$

where $f_+ = N_+/T_+$ and $f_- = N_-/T_-$ are the frequencies of earthquakes for "+" and "–" phases of tidal force correspondingly, N_+ and N_- are the numbers of earthquakes for "+" and "–" phases, T_+ and T_- are the total duration

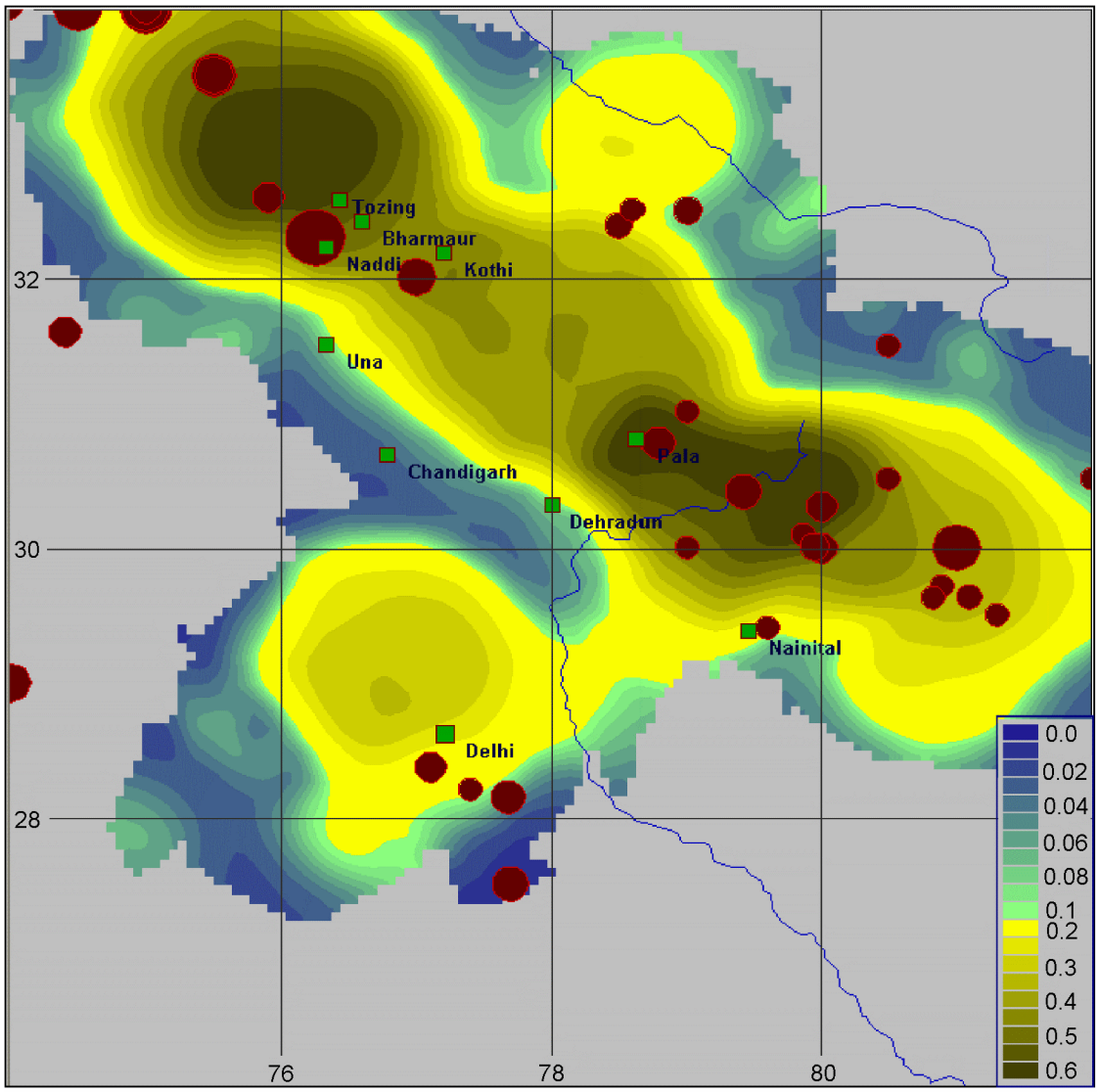

Figure 3. Spatial pattern of seismic activity $M = 3$ estimated by the WIHG earthquake catalogue from 01.01.1999 – 30.01.2005.

of intervals for "+" and "–" phase. The sign of s variable specifies in what phase ("+" or "–") earthquakes occur more often. Measure of s possesses statistical properties: if N_+ and N_- are sufficiently great, then value s has standard normal distribution and so its big values (for example, 2 or 3) are "significant", i.e. argue in favor of correlation between seismicity and tidal force.

[30] Earthquakes with the magnitudes $m \geq 2$ from 01.01. 1999 till 30.01.2005 were used to estimate the correlations. The maps of prevailing seismic activity for characteristics of tidal force F_r, F_{SN}, F_{WE}, F_h, $|F|$ and A_r were analyzed. For this purpose the territory under study is divided on square (in terms of degree measure) cells. If the number of earthquakes within the cell is more than 10, then the frequencies of earthquakes corresponding to "+" and "–" phases of the tidal characteristic are calculated. Thus signs "+" or "–" are assigned to the cells depending on prevalence either of two frequencies.

[31] Under close examination of the results some "positive" or "negative" cells form clusters of the cells. Such clusters are approximated by ellipses. Frequencies f_+, f_- and measure s are calculated for the seismic events which fit in the ellipses.

[32] As a result of the analysis the area **AI** which appeared

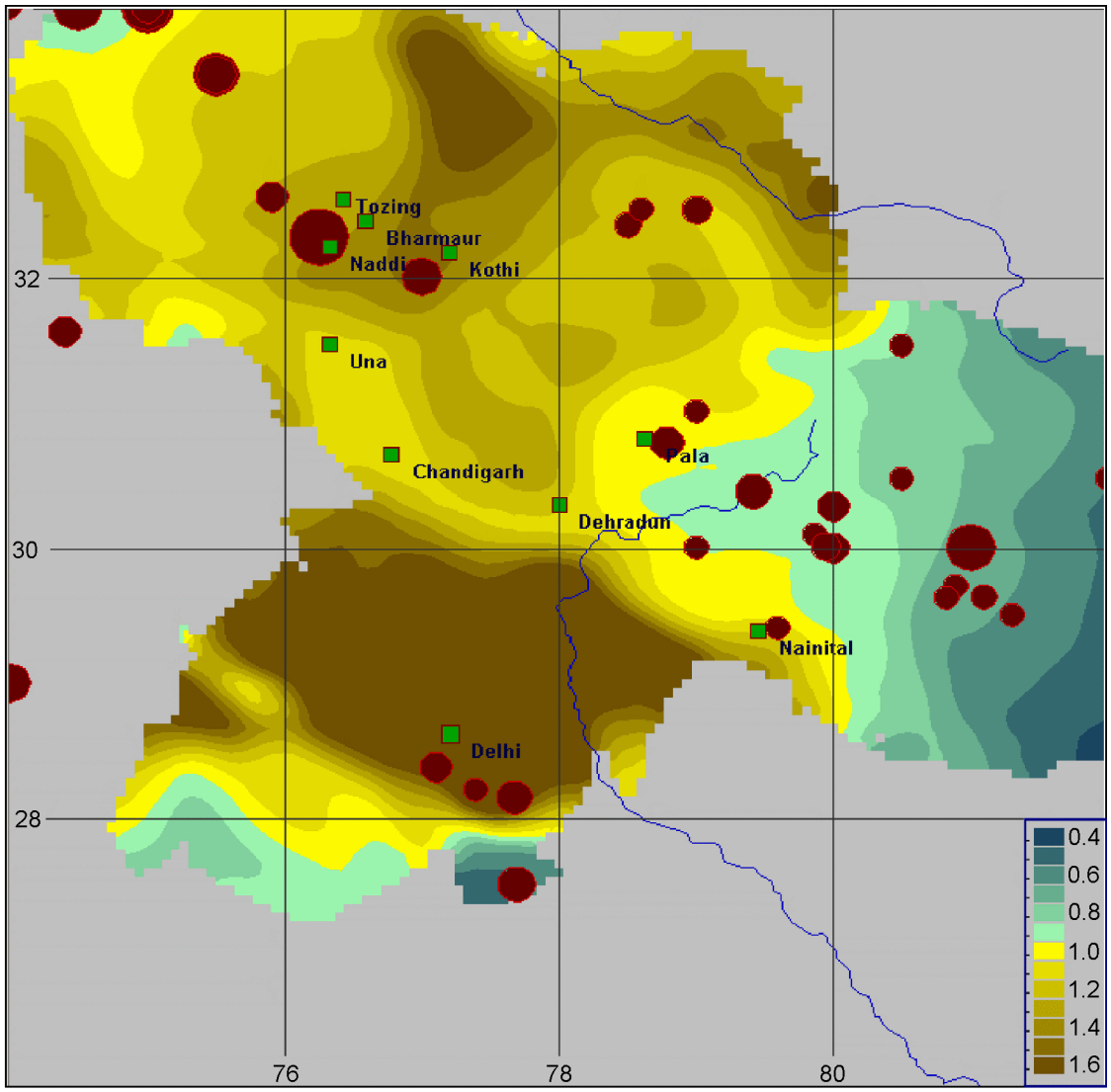

Figure 4. Spatial pattern of b-value $M = 3$ estimated by the WIHG earthquake catalogue from 01.01.1999 – 30.01.2005.

seismically sensitive to tidal force A_r is shown on Figure 6. This area includes 178 events, the ratio frequencies of earthquakes in "+" and "–" phases $f_+/f_- = 0.6$, $s = -3.5$. The size of statistics s in this area is high enough, that testifies to essential distinction between frequencies of earthquakes for two compared phases. Thus, frequency of earthquakes for negative phase tidal force A_r is raised (in comparison with positive phase of this characteristic). Similar correlations for other characteristics of tidal force were not revealed.

[33] The interpretation of this result is based on the assumption that a unidirectional action of the tectonic and tidal pressures increases probability the earthquake. We shall notice that vertical tidal force in a negative phase causes compression of the earth crust. Setting the intensity of earthquakes during a negative phase of characteristic A_r is raised, it is necessary to conclude, that area **AI** is in a condition of primary vertical tectonic compression.

6. Spatial Analysis of Relationship Between Strong Earthquakes With $M \geq 6$ and Digital Elevation Model

[34] Digital elevation model of the region under study and strong earthquakes $M > 6.0$ are represented at Figure 1. We

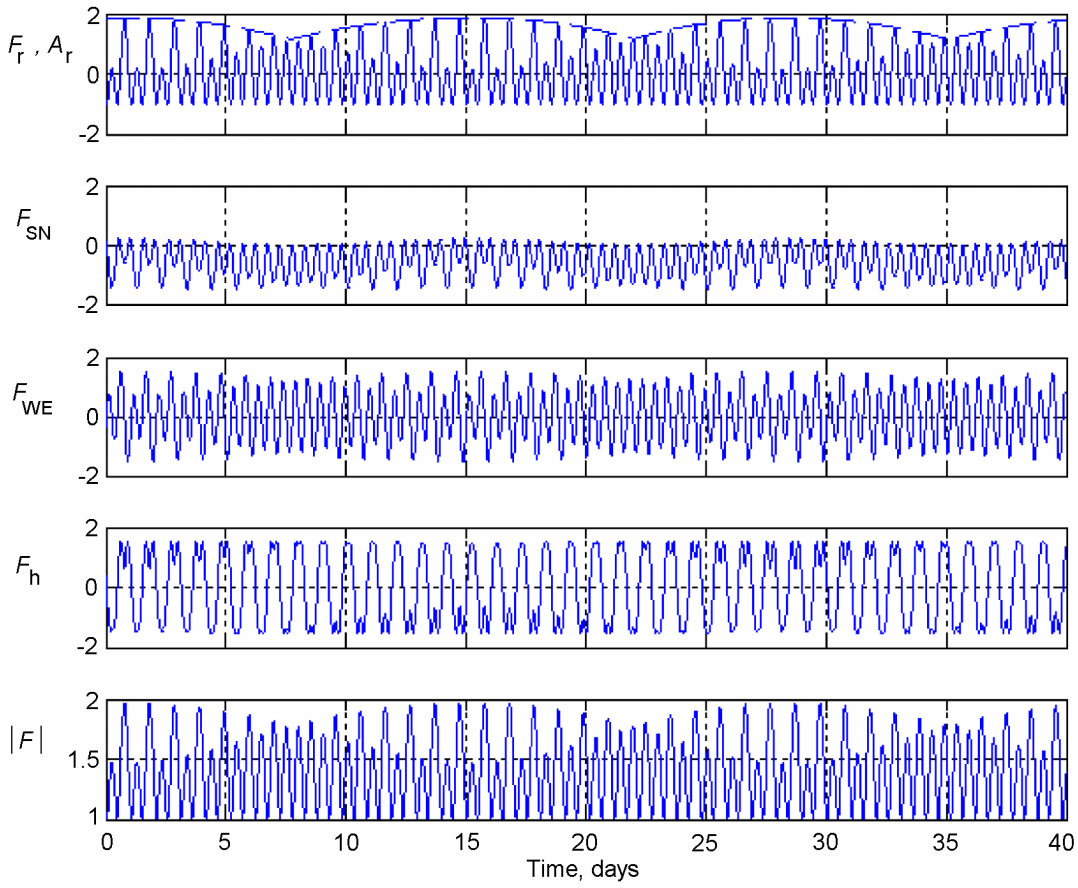

Figure 5. Time diagrams of tidal vector components for latitude 32°. F_r is vertical (radial) component, dashed line A_r is envelope for characteristic F_r, F_{SN}, F_{EW} are meridional and latitudinal horizontal components, F_h is the module of a vector of horizontal components, and $|F|$ is the module of a full vector of tidal force. The scale on a vertical is given in relative units.

can suggest that Himalayan seismicity is mostly correlated with heterogeneities of Earth crust, which are manifested by Earth surface relief. Taking into account this hypothesis we calculated root mean square (RMS) of the Earth surface elevations with moving window R=15 km (Figure 7). We can see that the most of Himalayan earthquakes with $M > 6.0$ are located in zone with RMS>500 m.

[35] This is the zone where Himalayan mid-crustal ramp under the southern Higher Himalaya has been proposed on the basis of various geophysical studies [*Gahalaut and Kalpna,* 2001; *Yeats and Thakur,* 1998]. Throughout Himalaya and mainly in NW Himalaya, a narrow belt between Higher and Lesser Himalaya shows intense seismic activity, the region is close to ramp and better known as Himalayan Seismic Belt (HSB). *Yeats and Thakur,* [1998] has given a fault-bend fold model where the megathrust drives southward and upward over the ramp and the axial surface of the fold is active at crustal sacle only. The central Himalaya moves southward as a fault bend fold due to slip by earthquakes that nucleate the detachment under Himalaya of this region. That study also shows maximum relief over the structural ramp indicating a high uplift rates over the ramp. Therefore a high uplift rates in the central Himalaya above the frontal ramp is due to thrust movement during megathrust earthquakes identified by recent compiled seismic catalogue.

7. Discussion

[36] Presently, most of the analysis is done for the seismic data of January 1999 to January 2005 with the improved quality of the catalogue for this period. The grid based mod-

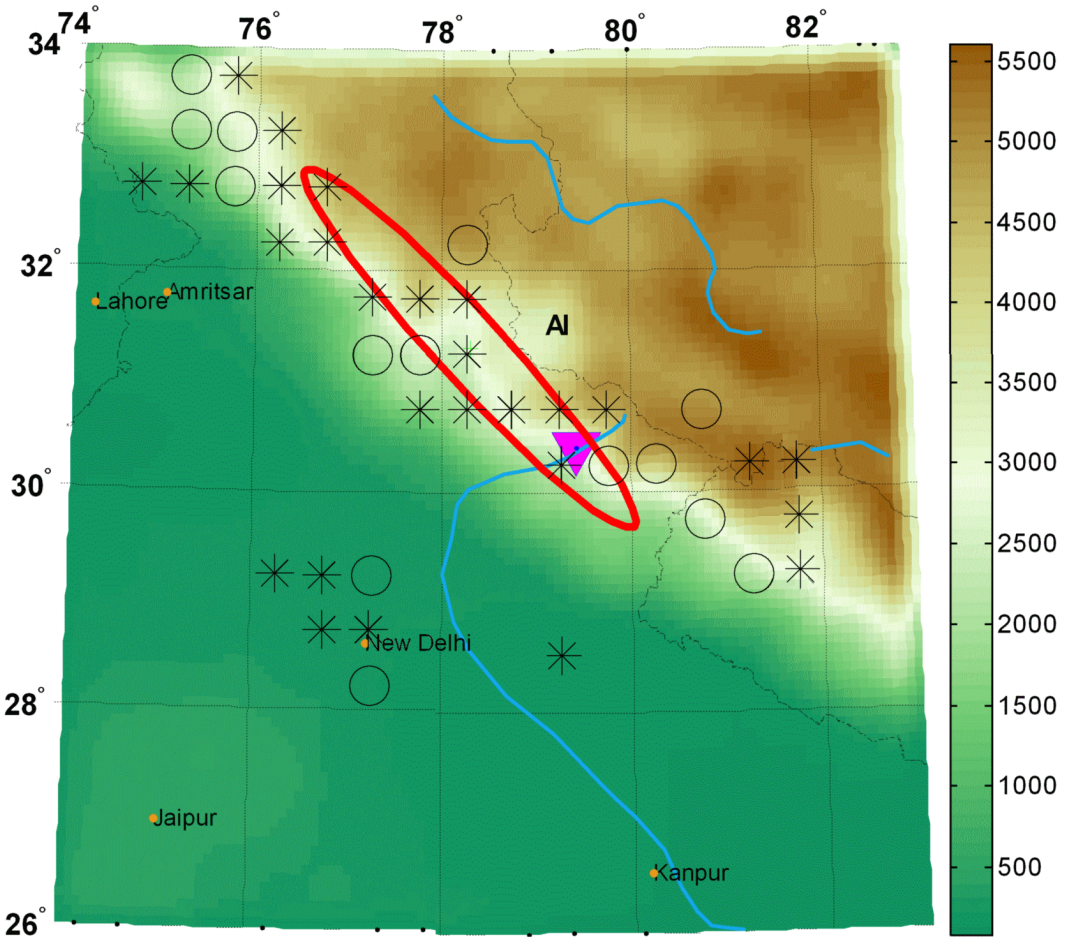

Figure 6. Area **AI** which is sensitive to the component A_r includes 178 events, $f_+/f_- = 0.6$, $s = -3.5$. Cells (size of $0.5^\circ \times 0.5^\circ$) with number of events more than 10 are shown: ◯ are the cells, for which $f_+ > f_-$; $*$ are the cells, for which $f_+ < f_-$. Symbol ▽ marks earthquake with magnitude 6.8 of 28 March 1999.

eling of spatial analysis of seismicity (Figure 2) shows that the region around Delhi has lowest value (2.0) of the minimal representative magnitudes, while its value is highest (2.6) in the region of Punjab reentrant and SW of Garhwal-Kumaon region. The seismic activity of earthquakes with $m = 3$ is highest to the SW of Garhwal-Kumaon region and lowest in the Delhi-Haridwar region (Figure 3), While the b-value pattern is opposite at these two regions (Figure 4). The b-value is around 0.5 for Kangra-Chamba region and less than 0.5 for the Garhwal-Kumaon region. The low b-value of these two regions can be stated that the regions have less capability to withstand the developing stress. The Lunar component of tidal force is compared with the seismic activity of the region in Figure 6 that shows the area **AI** seismically active to the daily variation of tidal force A_r. The level of statistics s in this area is high enough to testify essential distinction between frequencies of earthquakes for two compared phases. This result manifested that area **AI** is in a condition of primary vertical tectonic compression. The standard deviation of the Earth surface elevations (consequences of geotectonic deformation) with RMS value more than 500 m is positively correlated with the strong earthquakes $M \geq 6$ (Figure 7).

[37] **Acknowledgments.** This work was carried out under ILTP cooperation program. It was supported in part by ILTP, by the Russian Foundation for Basic Research, project no. 06-07-89139 and by Basic research program of Presidium of RAS No 15, section "Electronic Earth". We are grateful to colleagues in the projects for helpful discussions.

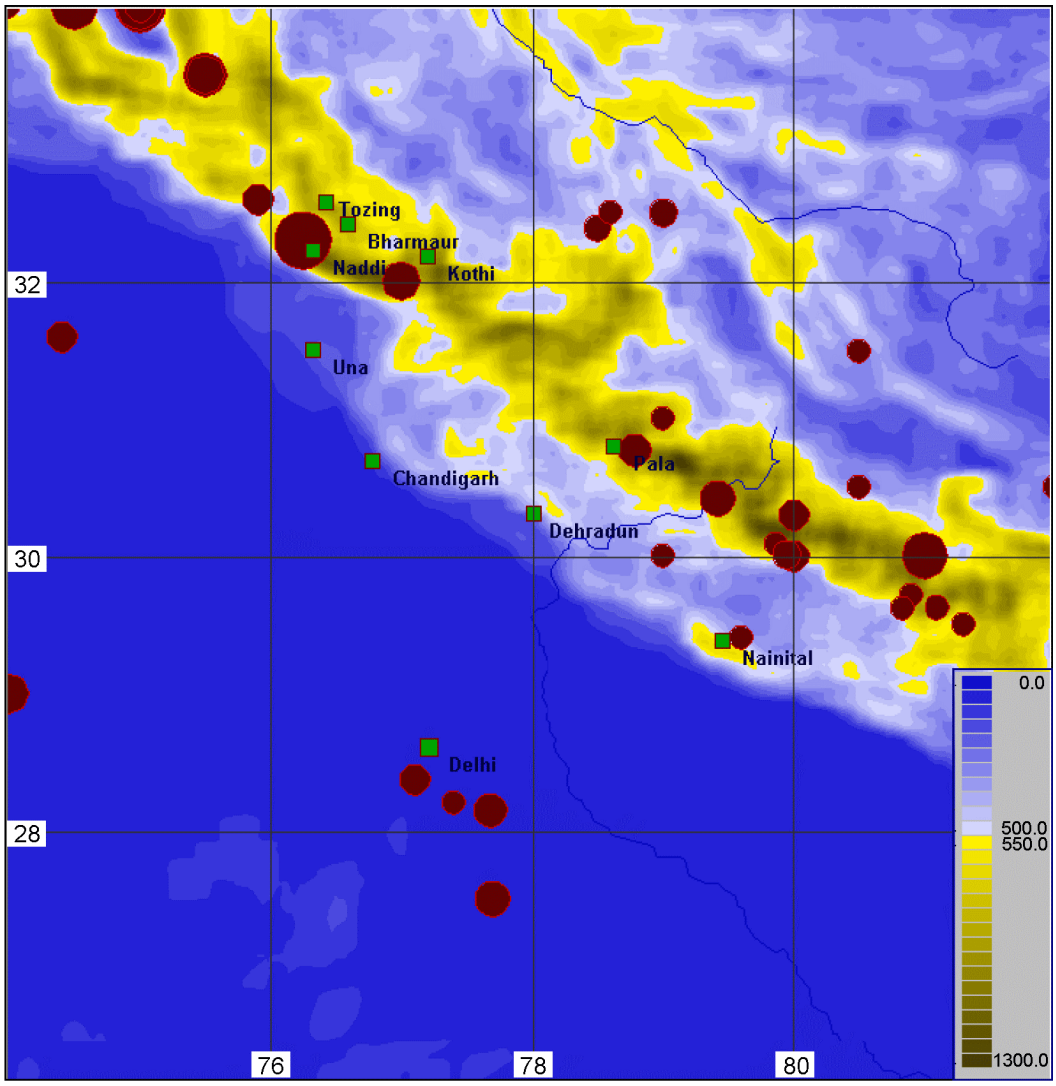

Figure 7. The grid-based model of root mean square of the Earth surface elevations with moving window R=15km and the epicenters with $M \geq 6.0$ of WIHG earthquake catalogue from 1552 – 30.01.2005.

References

Allegre, C., J., et al. (1984), Structure and evolution of the Himalaya-Tibet orogenic belt, *Nature, 307,* 17, doi:10.1038/307017a0.

Bollinger, L., F. Perrier, J.-P. Avouac, S. Sapkota, U. Gautam, and D. R. Tiwari (2007), Seasonal modulation of seismicity in the Himalaya of Nepal, *Geophys. Res. Lett., 34,* L08304.

Burg, J. P., M. Guiraurd, G. M. Chenn, and G. C. Li (1984), Himalayan metamorphism and deformations in the north Himalaya Belt (Southern Tibet, China), *Earth Planet. Sci. Lett., 69,* 391, doi:10.1016/0012-821X(84)90197-3.

Gahalaut, V. K., and Kalpna (2001), Himalayan mid-crustal ramp, *Curr. Sci., 81*(12), 1641.

Gitis, V. (2004), Experience of spatio-temporal seismotectonic data mining in multidisciplinary measurements, in *Proceedings of European Seismological Commission XXIX General Assembly,* p. 146, ESC, Potsdam,

Gitis, V., A. Dovgyallo, B. Osher, and T. Gergely (1998), GeoNet: an information technology for WWW on-line intelligent Geodata analysis, in *Proceedings of the 4th EC-GIS Workshop,* p. 124, Joint Research Centre of European Commission, Hungary.

Gitis, V., and B. Ermakov (2004), *Fundamentals of spatio-temporal forecasting in geoinformatics,* 256 pp., Fizmatlit, Moscow.

Gitis, V. G., B. V. Osher, S. A. Pirogov, A. V. Ponomarev, G. A. Sobolev, and E. F. Jurkov (1994), A System for Analysis of Geological Catastrophe Precursors, *Journal of Earthquake Prediction Research, 3,* 540.

Kayal, J. R. (2007), Recent large earthquakes in India: Seismotectonic Perspective, *IAGR Memoir, 10,* 189.

Le Fort, P. (1975), Himalaya: the collided range, present knowledge of the continent arc, *Am. J. Sci., 275,* 7.

Ni, J., and M. Barazangi (1984), Seismotectonics of the Himalayan collision zone: Geometry of the Underthrsuting Indian Plate beneath the Himalaya, *J. Geophys. Res., 89,* 1147.

Pisarenko, V. (1989), About frequency-magnitude relationship of earthquakes, in *Discret properties of geological environment,* p. 47, Nauka, Moscow.

Rao, N. P., P. Kumar, Kalpna, T. Tsukuda, and D. Ramesh (2006), The devastating Muzaffarabad earthquake of 8 October 2005: New insights into Himalayan seismicity and tectonics, *Gondwana Research, 9*(4), 365, doi:10.1016/j.gr.2006.01.004.

Seeber, L., and J. G. Arnbruster (1981), Great detachment earthquakes along the Himalayan arc and long forecasting, in *Earthquake Prediction – an international review,* vol. 4, p. 259, Am. Geophys. Union., Maurice Ewing Ser., Washington.

Smirnow, V. (1995), Earthquake recurrence and seismic regime parameters, *Volcanology and seismology,* no. 3, 59.

Thakur, V. C. (1992), *Geological Map of Western Himalaya,* 22 pp., Wadia Inst. Him. Geol., Dehradun.

Thakur, V. C., and S. Kumar (2002), Seismotectonics of Chamoli Earthquake of March 29, 1999 and Earthquake Hazard Assessment of Garhwal-Kumaon Region, NW Himalaya, *Himalayan Geology, 23*(1–2), 113.

Yeats, R. S., and V. C. Thakur (1998), Reassessment of earthquake hazard based on a fault-bend fold model of the Himalayan plate-boundary fault, *Curr. Sci., 74*(3), 220.

Yurkov, E., and V. Gitis (2005), Relation between Seismicity and Phases of Tidal Waves, *Izvestiya, Physics of the Solid Earth, 41*(4), 255.

B. Arora, S. Chabak, N. Kumar, Wadia Institute of Himalayan Geology, Dehradun, India

P. Baidya, India Meteorological Department, New Delhi, India

V. Gitis, E. Yurkov, Institute for Information Transmission Problems, RAS, Moscow, Russia (gitis@iitp.ru)